Evaluation of Micropolar Fluid Transport through Penetrable Medium: Effect of Flow and Thermal Slip

A.T. Akinshilo[*1], M.G. Sobamowo[1] and A. Adingwupu[2].
[1] Department of Mechanical Engineering, University of Lagos, Akoka-Yaba, Nigeria.
[2] Department of Mechanical Engineering, Igbinedion University, Edo, Nigeria.
*Corresponding author E-mail: ta.akinshilo@gmail.com.

Abstract

In this study, the micro polar fluid flow through penetrable walls under slip flow and thermal jump condition is examined. The Micropolar fluid accounts for the hydrodynamic limitation of the classical Navier Stokes model, it takes into consideration micro-structure of the fluid, local structure and micro rotation of fluid particles. Here the thermal exchange and mass transport of the micro polar fluid is studied considering transport conditions such as radiation, variable magnetism and nanoparticle concentration. The micropolar fluid flows into the channel and exits under slip velocity and temperature jump condition. The channel walls are assumed porous, fluid is incompressible, Newtonian and flowing steadily. The mechanics of the fluid is described by coupled, highly successive, nonlinear system of higher order partial differential equations transformed using appropriate similarity transform to ordinary differentials. These are analyzed adopting the Homotopy perturbation method of analysis. Results obtained from analysis shows quantitative increase of nanoparticles concentration from $1-4\%$ enhances thermal transfer, which effect is significant towards the lower plate. Similarly radiation increase reveals higher heat transfer while Reynolds parameter shows reducing heat transfer. Results obtained compared with similar literatures are in good agreement. Study finds good application in tribology, ferro fluids and arterial blood flow amongst other practical, yet relevant applications.

Keywords: Micropolar fluids; Thermal Radiation; Slip Flow; Thermal jump; HPM.

1. Introduction

The study of Micropolar fluid transport phenomena over the years cannot be over emphasized. As the Micropolar fluid accounts for the hydrodynamic limitation of the classical Navier Stokes model, this fluid takes into consideration micro-structure of the fluid, local structure and micro rotation of fluid particles. The model proposed by Eringen [1] to study the effect of this fluid can be explained considering the micro-rotation effect of fluid particles during flow. Similarly the study of micropolar heat transfer and flow through porous plates was studied by Aurangzaib et al. [2]. Transport of micropolar fluid was studied by Bank and Dash [3] through porous medium with the impact of magnetic field. Sheikholelami et al. [4] analyzed the micropolar fluid flow through porous medium with the aid of analytical methods. Pulsatile flow of magneto micropolar fluid on peristaltic motion through porous medium was investigated by Mekhar and Mohammed [5]. Viscous dissipation of micropolar fluid flowing past a stretching plate nonlinearly was investigated by Ahmad et al. [6]. Magnetic intensity influence on micropolar fluid was studied by Deo et al. [7] using a cylindrical tube with impermeable core. Newtonian and non-Newtonian analysis of flow was performed by Hatami and Jing [7] using semi analytical analysis. Micropolar magneto hydrodynamic convective flow due to deformable porous heated plate was studied by Trkyilmazoglu [8]. Flow and heat transfer was examined by Akinshilo [9] for injection nanofluid flow through expanding and contracting porous channel. Viscous dissipation and joule heating effect is investigated on the micropolar fluid flow by Lund et al. [10] flowing over a shrinking sheet. Heat and mass flow of micropolar fluid was analyzed using computational analysis by

Ahmad et al. [11]. Combined effect of absorption and heat generation on micropolar fluid under chemical reaction was presented by Damseh et al. [12] flowing over stretched permeable surface uniformly. Micropolar flow with nanoparticles was presented by Alizadeh et al. [13] under the influence of thermal radiation and constant magnetic field. Effect of heat flux applied uniformly and heat generation on micropolar fluid flowing vertically along a permeable plate was studied by Rahman et al. [14]. Nanofluid flows through parallel plates embedded with porous medium was studied by Akinshilo [15].

The importance of the nanoparticles during heat transfer cannot be overemphasized as it raises fluid thermal conductivity, consequently saving energy. This has stimulated researcher's interest in the application of the nanoparticles to fluid heat transfer. Hence water based single walled carbon nanotubes (SWCNTs) and multi walled carbon nanotubes (MWCNTs) particles non-Darcy flow was studied by Hayat et al. [16] having multiple slips. Intermolecular adhesive and cohesive forces sensitivity of MWCNTs incorporated into paraffin was presented by Yan et al. [17]. Tian et al. [18] studied the rheological behavior of hybrid MWCNTs and copper oxide nanofluid in a suspension of water and ethylene glycol. Pulsatile blood flow motion was modelled in elastic artery by Sharifzadeh et al. [19] for biomedical applications. Dynamics of molecules on ferro nanofluid considering barrier effects was analyzed by Fazinpour et al. [20] in the presence of external, time dependent magnetic field. Yian et al. [21] investigated the rheological properties of hybrid MWCNTs and TiO_2 nanofluid. Type of nanoparticle, base temperature, size and shape was studied on the convective boundary layer of nanofluid by Zakari et al. [22]. Thermal and mass transfer effect on convective boundary layer was studied by [23-26] through transport medium.

Since problems of these types are usually nonlinear in nature, which demands boundary value coupled system higher order models. Analyzing, investigating and examination of the mechanics of the micropolar flow transport and thermal transfer requires either numerical or analytical methods as suitable methods of analysis utilized by researchers over the years [27-49]. These methods of analysis includes the Akbari-Ganji method [AGM], differential transform method [DTM], method of weighted residuals (Garlerkins, collocation and least squares), Adomian decomposition method [ADM], Homotopy analysis methods [HAM] and variation of iteration method [VIM] amongst others. The AGM is an iterative method which is time consuming for systems of strongly nonlinear models, the errors of approximation due to iteration is low. Computation stencils are required for the analysis of HAM in the determination of its initial or guess term, auxiliary function and parameter. This results in large computational cost, the HAM as the ability to solve complex ordinary or partial system of equations. VIM and method of weighted residuals suffers from errors of approximation but method of analysis are relatively simple. The DTM requires the use of programmable tools such as Matlab or Maple in handling strongly nonlinear analysis. The analysis of ADM involves solving adomian polynomials which are rigorous for nonlinear equations. Homotopy perturbation method [HPM] is selected in this study as the preferred analytical scheme to analyze the problem. This is owing to a rapid rate of convergence of approximate analytical solutions, accuracy and reliability of data obtained from investigation of the coupled system of nonlinear mechanics governing mass and heat transfer.

With respect to the above, this study investigates the effect of velocity slip and thermal jump on the steady micropolar fluid transport through penetrable medium. The system of mechanics of fluid transport is described by nonlinear models and analyzed using the Homotopy perturbation method with obtained solutions validated against the Fourth order Runge Kutta Fehlberg numerical method. This proves to be in excellent agreement, increasing confidence in obtained results.

2. Problem Description and Governing Equations

The two dimension micropolar steady flow in a horizontal channel is considered in this section. The micropolar fluid flows into the channel and exits under slip velocity and temperature jump condition. As described in the Fig. 1, the bottom wall is defined as T_1 and the top wall temperature is indicated as T_2. The channel walls are assumed porous, fluid is incompressible, Newtonian and flowing steadily. The parallel surface to the channel wall is the x axis and normal to the wall is the y axis. The walls of the channels are located at $y = \pm h$ .Thermal equilibrium condition is assumed between the base fluid and nanoparticles. Velocity slip and thermal jump influence on flowing micropolar fluid particles under constantly applied magnetic field is considered. Subject to the above illustrations, governing equations for momentum and energy are presented as follows [13]:

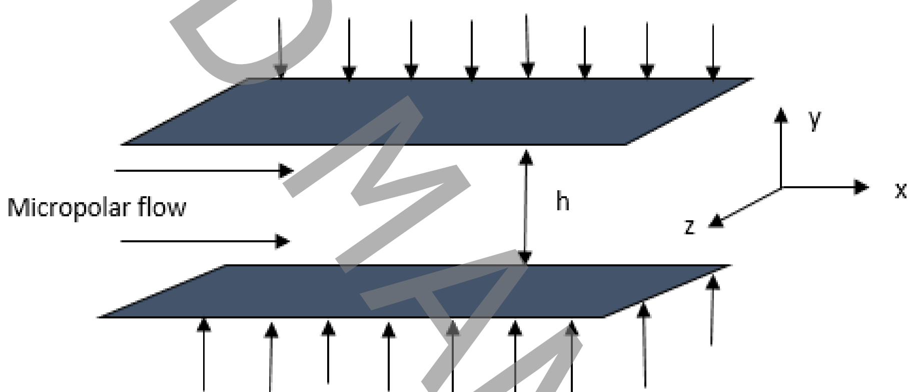

Fig. 1. Physical model of problem.

$$\frac{\partial u}{\partial x}+\frac{\partial v}{\partial y}=0 \tag{1}$$

$$\rho_{nf}\left(u\frac{\partial u}{\partial x}+v\frac{\partial u}{\partial y}\right)=-\frac{\partial p}{\partial x}+\left(\mu_{nf}+k\right)\left(\frac{\partial^2 u}{\partial x^2}+\frac{\partial^2 u}{\partial y^2}\right)+k\frac{\partial N}{\partial y}-\sigma_f B_0^2 u \tag{2}$$

$$\rho_{nf}\left(u\frac{\partial v}{\partial x}+v\frac{\partial v}{\partial y}\right)=-\frac{\partial p}{\partial y}+\left(\mu_{nf}+k\right)\left(\frac{\partial^2 v}{\partial x^2}+\frac{\partial^2 v}{\partial y^2}\right)-k\frac{\partial N}{\partial x} \tag{3}$$

$$\rho_{nf}\, j\left(u\frac{\partial N}{\partial x}+v\frac{\partial N}{\partial y}\right)=-k\left(2N+\frac{\partial u}{\partial y}-\frac{\partial v}{\partial x}\right)+\gamma_{nf}\left(\frac{\partial^2 N}{\partial x^2}+\frac{\partial^2 N}{\partial y^2}\right) \tag{4}$$

$$u\frac{\partial T}{\partial x}+v\frac{\partial T}{\partial y}=\frac{k_{nf}}{\left(\rho C_p\right)_{nf}}\left(\frac{\partial^2 T}{\partial x^2}+\frac{\partial^2 T}{\partial y^2}\right)-\frac{1}{\left(\rho C_p\right)_{nf}}\frac{\partial q_{rad.}}{\partial y} \quad (5)$$

Where the vortex viscosity is given as k, viscosity spin gradient is $\gamma nf=\left(\mu nf+k/2\right)j$, directional velocities in x and y direction are u and v respectively, Pressure is P, Temperature is T, magnetic field is B_o, Micro rotation velocity is N, micro-inertia density is j and qrad is the heat flux radiation and σf is the electrical fluid conductivity.

The Rooseland approximation for radiation is defined as Eqs. [50-51]

$$q_{rad.}=-\left(4\sigma^*/3k_{nf}^*\right)\frac{\partial T^4}{\partial y}. \quad (6)$$

Here the constant of Stefan Boltzmann is given as σ^* and the nanofluid mean absorption coefficient is k_{nf}^*. It is further assumed that temperature difference within flow is such that Taylor series may expand T^4. Simplifying the terms, we obtain

$$T^4\cong 4T_\infty^3 T-3T_\infty^4. \quad (7)$$

Therefore, Eq. (5) is reduced to:

$$u\frac{\partial T}{\partial x}+v\frac{\partial T}{\partial y}=\frac{k_{nf}}{\left(\rho C_p\right)_{nf}}\left(\frac{\partial^2 T}{\partial x^2}+\frac{\partial^2 T}{\partial y^2}\right)+\frac{16\sigma^* T_\infty^3}{3k_{nf}^*\left(\rho C_p\right)_{nf}}\frac{\partial^2 T}{\partial y^2} \quad (8)$$

The effective fluid viscosity of the nanofluid is μnf, nanofluid effective density is ρnf, nanofluid heat capacity is $\left(\rho nf\right)_{nf}$ and the nanofluid thermal conductivity is knf are given as:

$$\begin{aligned}
&\rho_{nf}=\left(1-\phi\right)\rho_f+\phi\rho_s,\\
&\left(\rho C_p\right)_{nf}=\left(1-\phi\right)\left(\rho C_p\right)_f+\phi\left(\rho C_p\right)_s,\\
&\mu_{nf}=\frac{\mu_f}{\left(1-\phi\right)^{2.5}},\\
&\frac{k_{nf}}{k_f}=\frac{k_s+2k_f-2\phi\left(k_f-k_s\right)}{k_s+2k_f+2\phi\left(k_f-k_s\right)}.
\end{aligned} \quad (9)$$

With appropriate boundary conditions given as:

$$\begin{aligned}
&u=\beta_1\frac{\partial u}{\partial y}\quad v=0\quad N=-s\left.\frac{\partial u}{\partial y}\right|_{y=0}\quad T=\gamma_1\frac{\partial T}{\partial y}+T_0\quad \text{At}\quad y=0,\\
&u=-\beta_1\frac{\partial u}{\partial y}\quad v=v_0,\quad N=-s\left.\frac{\partial u}{\partial y}\right|_{y=h}\quad T=-\gamma_1\frac{\partial T}{\partial y}+T_h\quad \text{At}\quad y=+h.
\end{aligned} \quad (10)$$

Here injection flows occurs at $V_0 < 0$ and suction flows occurs at $V_0 > 0$. The velocity slip is represented as β_1 and the thermal slip is denoted as γ_1. The rotational degree of the microelements near the walls and boundary parameter is s. For non-rotation close to the boundary wall, s=0. This condition corresponds to concentrated particle flows. Other similar cases have been considered by researchers such as $s = 0.5$ and $s = 1$. These connotes weak and turbulent flow conditions respectively. The nondimensionalized parameters are introduced as:

$$\begin{aligned} &\eta = \frac{y}{h}, \quad u = -\frac{v_0 x}{h} f'(\eta), \quad N = \frac{v_0 x}{h^2} g(\eta), \\ &v = v_0 f(\eta), \quad \theta = (T - T_1)/(T_2 - T_1). \end{aligned} \tag{11}$$

Given $T_2 = T_1 + Ax$, where A is a constant.

By substituting T$_2$ into the governing model of equations and pressure gradient is eliminated. Eqs. (2)- (4) and (8) are transformed into the following system of coupled nonlinear equations:

$$\begin{aligned} &\left(1 + (1-\phi)^{2.5} K\right) f^{iv} - (1-\phi)^{2.5} K g'' \\ &\quad - \left(1 - \phi + \frac{\rho_s}{\rho_f}\phi\right)(1-\phi)^{2.5} \mathrm{Re}\left(f f''' - f' f''\right) - (1-\phi)^{2.5} M f'' = 0 \end{aligned} \tag{12}$$

$$\begin{aligned} &\left(1 + \frac{(1-\phi)^{2.5}}{2} K\right) g'' + (1-\phi)^{2.5} K \left(f'' - 2g\right) \\ &\quad - \left(1 - \phi + \frac{\rho_s}{\rho_f}\phi\right)(1-\phi)^{2.5} \mathrm{Re}\left(f g' - g f'\right) = 0 \end{aligned} \tag{13}$$

$$\theta'' + \left((1-\phi) + \frac{(\rho C_p)_s}{(\rho C_p)_f}\phi\right)\left(\frac{3}{3+4N}\right)\frac{k_f}{k_{nf}} \Pr \mathrm{Re}\left(f'\theta - f\theta'\right) = 0 \tag{14}$$

Adopting the relevant boundary conditions

$$\begin{aligned} &f(0) = 0, \quad f'(0) = \beta f'', \quad f'(1) = -\beta f'', \quad f(1) = 1, \\ &g(0) = 0, \quad g(1) = 0, \\ &\theta(0) = 1 + \gamma\theta', \quad \theta(1) = -\gamma\theta'. \end{aligned} \tag{15}$$

Where Reynold parameter is Re given $Re < 0$ corresponds to injection flows while $Re > 0$ corresponds to suction flows, magnetic parameter is M, micropolar parameter is given as K, radiation parameter is N. These parameters are defined as follows:

$$\begin{aligned} &\mathrm{Re} = \rho_f v_0 h / \mu_f, \quad \Pr = \mu_f C_{p,f} / k_f, \quad N = 4\sigma^* T_\infty^3 / k_{nf} k_{nf}^*, \\ &M = \sigma_f B_0^2 h^2 / \mu_f, \quad K = k / \mu_f, \quad j = h^2. \end{aligned} \tag{16}$$

Other important engineering parameters of interest is the Nusselt number which is specified as follows:

$$Nu^* = -\left(\frac{h}{k_f\left(T_2 - T_1\right)}\right)\left(k_{nf} + \frac{16\sigma^* T_\infty^3}{3k_{nf}^*}\right)\frac{\partial T}{\partial y}\bigg|_{y=-h} \tag{17}$$

In terms of (9) and (11), we gain:

$$Nu = \left|\frac{k_{nf}}{k_f}\left(1 + \frac{4}{3}N\right)\theta'(-1)\right| \tag{18}$$

Table 1. Thermophysical properties of nanofluid Alizadeh et. al. [13].

	$\rho\left(Kg/m^3\right)$	$C_p\left(J/KgK\right)$	$K\left(w/mk\right)$
Copper (Cu)	8933	385	401
Water	997.1	4179	0.613

2.1 Application of the Homotopy Perturbation Method

Here the micropolar fluid flow through penetrable walls under slip and thermal jump condition are examined. The micropolar fluid flows steadily considering magnetic field and thermal transport. The mechanics of rotating particle flow is described using nonlinear coupled systems of higher order equations, these are analyzed utilizing the Homotopy perturbation method (HPM). Whose principles and fundamentals has been extensively discussed by Sobamowo and Akinshilo [45]. The HPM been an analytical method with fast rate of convergence, coupled with procedural stability is the selected method adopted to solve the system of coupled nonlinear model of higher differential. Therefore, constructing the Homotopy the governing equations Eqs. (12)- (14) are expressed as:

$$H_1(\mathrm{p},\eta) = (1-p)\left[\frac{d^4 f}{\partial\eta^4}\right] + p\left[\begin{array}{l}\dfrac{d^4 f}{d\eta^4} - (1-\phi)^{2.5}K\dfrac{d^2 g}{d\eta^2} - \left(1-\phi+\dfrac{\rho s}{\rho f}\phi\right)(1-\phi)^{2.5}\,\mathrm{Re}\left(f\dfrac{d^3 f}{d\eta^3} - f\dfrac{d^2 f}{d\eta^2}\right)\\ -(1-\phi)^{2.5}M^2\dfrac{d^2 f}{d\eta^2}\end{array}\right]$$
$$/\left(1+(1-\phi)^{2.5}K\right) = 0 \tag{19}$$

$$H_2(p,\eta) = (1-p)\left[\frac{d^2 g}{d\eta^2}\right] + p\left[\begin{array}{l}\dfrac{d^2 g}{d\eta^2} - (1-\phi)^{2.5}K\left(\dfrac{d^2 f}{d\eta^2} - 2g\right) - \left(1-\phi+\dfrac{\rho s}{\rho f}\phi\right)\\ (1-\phi)^{2.5}\,\mathrm{Re}\left(f\dfrac{dg}{d\eta} - g\dfrac{df}{d\eta}\right)\end{array}\right] / \left(1+\frac{(1-\phi)^{2.5}}{2}K\right) = 0 \tag{20}$$

$$H_2(p,\eta)=(1-p)\left[\frac{d^2\theta}{d\eta^2}\right]+p\left[\frac{d^2\theta}{d\eta^2}+\left((1-\phi)+\frac{(\rho C_p)_s}{(\rho C_p)_f}\phi\right)\left(\frac{3N}{3N+4}\right)\frac{k_f}{k_{nf}}\Pr\mathrm{Re}\left(\frac{df}{d\eta}\theta-f\frac{d\theta}{d\eta}\right)\right]=0 \quad (21)$$

Selecting power series of velocity and temperature profiles yields

$$f=P^0f_0+P^1f_1+P^2f_2+....... \quad (22a)$$

$$g=P^0g_0+P^1g_1+P^2g_2+....... \quad (22b)$$

$$\theta=P^0\theta_0+P^1\theta_1+P^2\theta_2+....... \quad (22c)$$

Eq. (22a) is substituted into (19) and selected at the various order yields

$$p^0:\frac{d^4f_0}{d\eta^4} \quad (23)$$

$$p^1:\left[\begin{array}{l}\frac{d^4f_1}{d\eta^4}-(1-\phi)^{2.5}K\frac{d^2g_0}{d\eta^2}-\left(1-\phi+\frac{\rho s}{\rho f}\phi\right)(1-\phi)^{2.5}\mathrm{Re}\left(f_0\frac{d^3f_0}{d\eta^3}-f_0\frac{d^2f_0}{d\eta^2}\right)\\-(1-\phi)^{2.5}M^2\frac{d^2f_0}{d\eta^2}\end{array}\right]/\left(1+(1-\phi)^{2.5}K\right) \quad (24)$$

$$p^2:\left[\begin{array}{l}\frac{d^4f_2}{d\eta^4}-(1-\phi)^{2.5}K\frac{d^2g_1}{d\eta^2}-\left(1-\phi+\frac{\rho s}{\rho f}\phi\right)(1-\phi)^{2.5}\mathrm{Re}\,f_0\frac{d^3f_1}{d\eta^3}+\left(1-\phi+\frac{\rho s}{\rho f}\phi\right)(1-\phi)^{2.5}\mathrm{Re}\,f_0\frac{d^2f_1}{d\eta^2}-\\(1-\phi)^{2.5}M\frac{d^2f_1}{d\eta^2}\end{array}\right]/\left(1+(1-\phi)^{2.5}K\right) \quad (25)$$

Eq. (22b) is substituted into (20) and selected at the various order yields

$$p^0:\frac{d^2g}{d\eta^2} \quad (26)$$

$$p^1:\left[\begin{array}{l}\frac{d^2g_1}{d\eta^2}-(1-\phi)^{2.5}K\left(\frac{d^2f_0}{d\eta^2}-2g_0\right)-\left(1-\phi+\frac{\rho s}{\rho f}\phi\right)\\(1-\phi)^{2.5}\mathrm{Re}\left(f_0\frac{dg_0}{d\eta}-g_0\frac{df_0}{d\eta}\right)\end{array}\right]/\left(1+\frac{(1-\phi)^{2.5}}{2}K\right) \quad (27)$$

$$p^2:\left[\frac{\mathrm{d}^2 g_2}{d\eta^2}+(1-\phi)^{2.5}K\frac{\mathrm{d}^2 f_1}{d\eta^2}-2g_1-\left(1-\phi+\frac{\rho s}{\rho f}\phi\right)(1-\phi)^{2.5}\operatorname{Re} f_0\frac{dg_1}{d\eta}+\left(1-\phi+\frac{\rho s}{\rho f}\phi\right)(1-\phi)^{2.5}\operatorname{Re} g_0\frac{df_1}{d\eta}\right]/\left(1+\frac{(1-\phi)^{2.5}}{2}K\right) \tag{28}$$

Eq. (22c) is substituted into (21) and selected at the various order yields

$$p^0:\frac{d^2\theta_0}{d\eta^2} \tag{29}$$

$$p^1:\frac{d^2\theta}{d\eta^2}+\left((1-\phi)+\frac{(\rho C_p)_s}{(\rho C_p)_f}\phi\right)\left(\frac{3N}{3N+4}\right)\frac{k_f}{k_{nf}}\Pr\operatorname{Re}\left(\frac{df}{d\eta}\theta-f\frac{d\theta}{d\eta}\right) \tag{30}$$

$$p^2:\frac{\mathrm{d}^2\theta_2}{d\eta^2}+\left((1-\phi)+\frac{(\rho C_p)_s}{(\rho C_p)_f}\phi\right)\left(\frac{3N}{3N+4}\right)\frac{k_f}{k_{nf}}\Pr\operatorname{Re}\left(\frac{df_0}{d\eta}\theta_1-f_0\frac{d\theta_1}{d\eta}\right) \tag{31}$$

Boundary condition for leading order is given as

$$f_0(0)=0\quad \frac{df_0}{d\eta}(0)=\beta\frac{df^{2}_{0}}{d\eta^2}\quad \frac{df_0}{d\eta}(1)=-\beta\frac{d^2 f_0}{d\eta^2}\qquad f_0(1)=1 \tag{32}$$

Solving Eq. (23) using the leading order boundary condition Eq. (32) yields

$$f_0=\frac{2A\eta^3-3A\eta^2+6A\beta\eta}{6\beta-1} \tag{33}$$

Boundary condition for leading order is given as

$$\mathrm{g}_0(0)=0,\mathrm{g}_0(1)=0 \tag{34}$$

Solving Eq. (26) using the leading order boundary condition Eq. (34) yields

$$g_0=\frac{\eta+(\gamma-1)}{2\gamma-1} \tag{35}$$

Boundary condition for leading order is given as

$$\theta_0(0)=1+\gamma\frac{d\theta_0}{d\eta},\theta_0(1)=-\gamma\frac{d\theta_0}{d\eta} \tag{36}$$

Solving Eq. (29) using the leading order boundary condition Eq. (36) yields

$$\theta_0=0 \tag{37}$$

Boundary condition for first order is given as

$$f_1(0)=0\quad \frac{df_1}{d\eta}(0)=\beta\frac{df^{2}_{1}}{d\eta^2}\quad \frac{df_1}{d\eta}(1)=-\beta\frac{d^2 f_1}{d\eta^2}\qquad f_1(1)=1 \tag{38}$$

Solving Eq. (24) using the first order boundary condition Eq. (38) yields

$$f_1 = \eta^5(((9A^2\beta \operatorname{Re}\rho_f)/2 - (9A^2\beta \operatorname{Re}\rho_f\phi)/2 + 9A^2BRE\phi\rho_s)/2/(5\rho_f(6\beta-1)^2(K(1-\phi)^{2.5}+1)) - ((AM \rho_f(1-\phi)^{2.5} - 3A\beta M\rho_f(1-\phi)^{2.5}/(5\rho_f(6\beta-1)^2(K(1-\phi)^{2.5}+1)(m+1))) + \eta^3((S(70A\rho_f - 840A\beta m\rho_f + 70AK\rho_f(1-\phi)^{2.5} - 840A\beta m\rho_f + 70AK\rho_f(1-\phi)^{2.5} + 7AM\rho_f(1-\phi)^{2.5} - 840A\beta K\rho_f(1-\phi)^{2.5} - 77A\beta M\rho_f(1-\phi)^{2.5} + \ldots \quad (39)$$

Boundary condition for first order is given as

$$g_1(0) = 0, g_1(1) = 0 \quad (40)$$

Solving Eq. (27) using the first order boundary condition Eq. (40) yields

$$g_1 = ((18\,\mathrm{ANPrRe}k_f\,\rho_{cf} - 18AN\Pr\operatorname{Re}k_f\rho_{cf} + 18AN\Pr\operatorname{Re}k_f\rho_{cs}\phi)/(4k_{nf}\rho_{cf}(6\beta-1)(3N+4)(4R+3)(2\gamma-1) - (18AN\Pr\operatorname{Re}k_f\rho_{cf} - 18AN\Pr\operatorname{Re}k_f\rho_{cf}\phi + 18AN\Pr\operatorname{Re}k_f\rho_{cs}\phi)/(8k_{nf}\rho_{cs}\phi)/(8k_{nf}\rho_{cf}(6\beta-1)(3N+4)+(4R+3)))\eta^4 - ((9AN\Pr\operatorname{Re}k_f\rho_{cf} - 9AN\Pr\operatorname{Re}k_f\rho_{cf} + \ldots \quad (41)$$

Boundary condition for first order is given as

$$\theta_1(0) = 1 + \gamma\frac{d\theta_1}{d\eta}, \theta_1(1) = -\gamma\frac{d\theta_1}{d\eta} \quad (42)$$

Solving Eq. (30) using the first order boundary condition Eq. (42) yields

$$\theta_1 = -((12AK(12\beta-2)(1-\phi)^{2.5} - 12AK(K-6\beta K)(\phi-1)^5)\eta^3)/(3(12\beta-2)^2 + 3(K-6\beta K) + ((12AK(12\beta-2)(1-\phi)^{2.5} - 12AK(K-6-\beta K)(\phi-1)^5)\eta^2)/(2(12\beta-2)^2 + \ldots \quad (43)$$

The Eqs (25), (28) and (31) second order solutions p^2 for $\mathrm{F}(\eta)$, $\mathrm{g}(\eta)$ and $\theta(\eta)$ were too voluminous. However they were represented in results validation and the graphical figures. Hence, expressions for final flow and heat transfer are given as:

$$\mathrm{f}(\eta) = f_0(\eta) + f_1(\eta) + f_2(\eta) \quad (44)$$

$$\mathrm{g}(\eta) = g_0(\eta) + g_1(\eta) + g_2(\eta) \quad (45)$$

$$\theta(\eta) = \theta_0(\eta) + \theta_1(\eta) + \theta_2(\eta) \quad (46)$$

3.0 Result and Discussions

In this section, the result obtained from the analytical investigation of the coupled nonlinear higher order model for flow and thermal transport are reported graphically. At higher quantitative values of Reynolds parameter for velocity, the fluid flow is impeded and thermal transfer is enhanced. In the same vein, no effect is noticed on the micro rotation profile. The Fig. 2 reveals the effect of enhanced micropolar parameter on fluid transport through the penetrable medium, as observed this depicts steady increase of fluid particle velocity from the lower plate to the upper plate. This can be physically explained owing to decreasing momentum boundary layer thickness, as freely colliding rotating particles reduces kinematic viscosity. Also the effect of micropolar fluid flow under constant magnetic field effect is seen in Fig. 3, this reveals applied magneto hydrodynamic influence on fluid particle motion is enhanced until about the mid plate $\eta = 0.5$ (not determined accurately) thereafter a reverse in flow trend towards the upper plate is seen. This phenomenon is as a result of resistive force boundary forces known as Lorentz force towards channel boundary which limits fluid flow, consequently intensity of magnetic field abates.

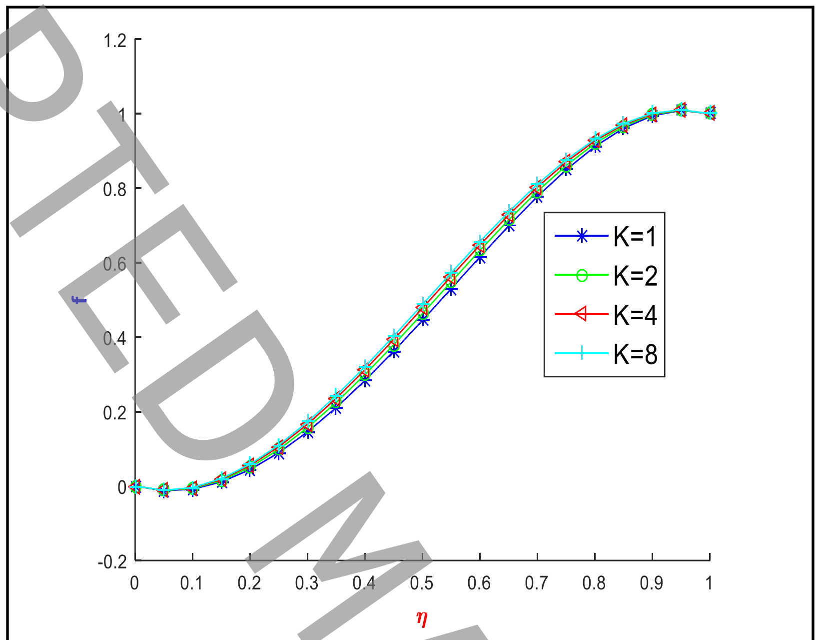

Fig. 2. Effects of micro polar parameter (K) on velocity.

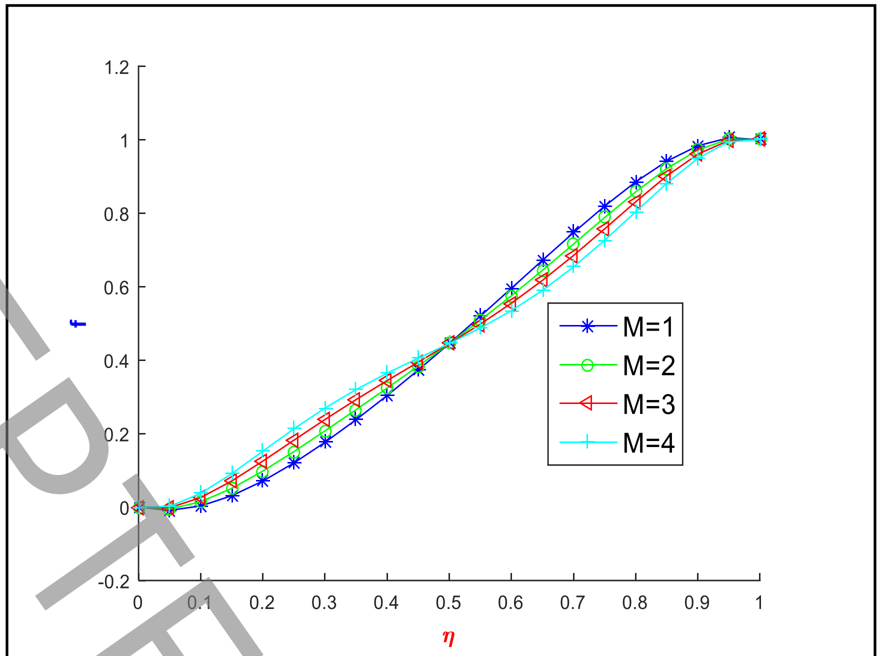

Fig. 3. Effects of magnetic parameter (M) on velocity.

Thermal effect on the micropolar flow is observed in Figs. 4-6. As observed from Fig. 4 improving Prandtl number effect is seen on the thermal distribution. As seen high Prandtl number increases thermal distribution along the flow medium as thermal boundary layer improves due to temperature gradient at channel surface. Increasing effect of radiation is observed in Fig. 5, as the micropolar fluid flows through the channel, this reveals high radiation abate temperature. Due to rapid exchange of heat during the flow transport, hence improved heat transfer diminishes thermal layer thickness .Concentration of nanoparticle in micropolar fluid is analyzed in Fig. 6. Increasing concentration of nanoparticles of copper causes high energy exchange as the fluid flows reduces thermal boundary layer thickness for the micropolar nano mix. This improves heat transfer which is significant at the lower plate.

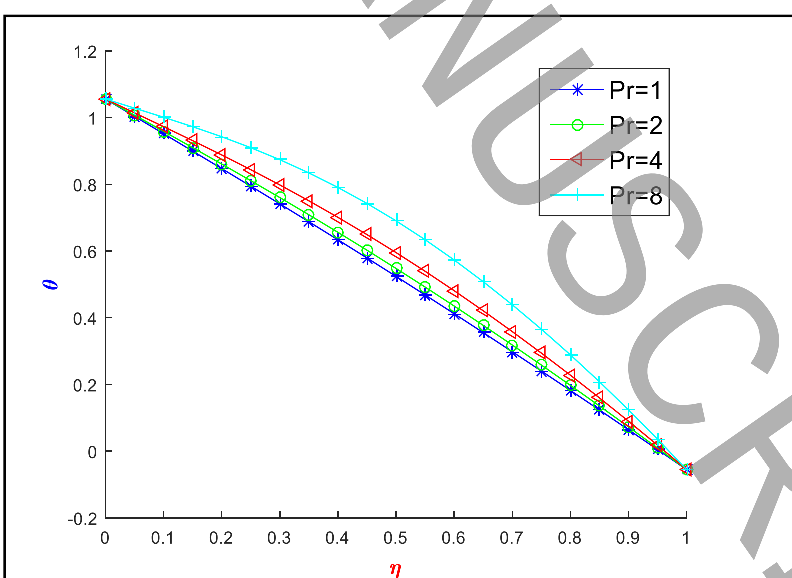

Fig. 4. Effects of Prandtl number (Pr) on temperature.

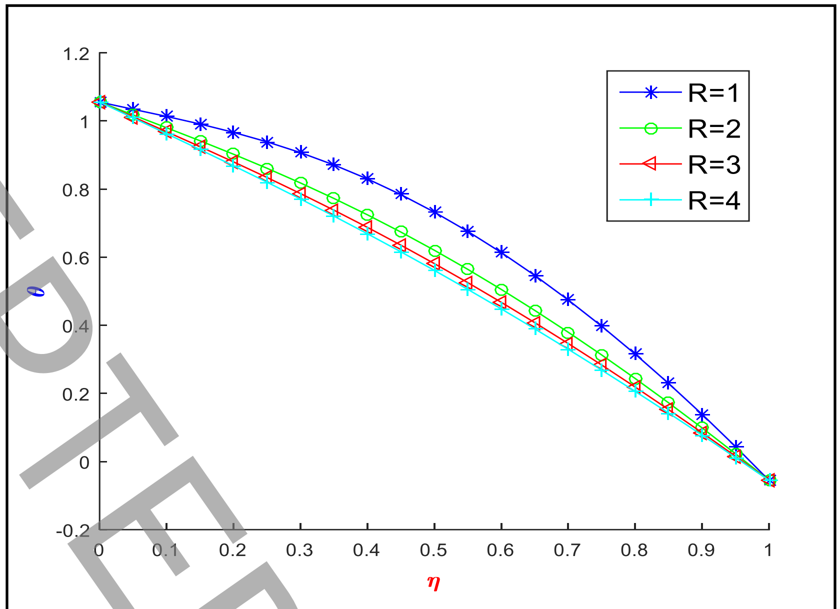

Fig. 5. Effects of Radiation parameter (R) on temperature.

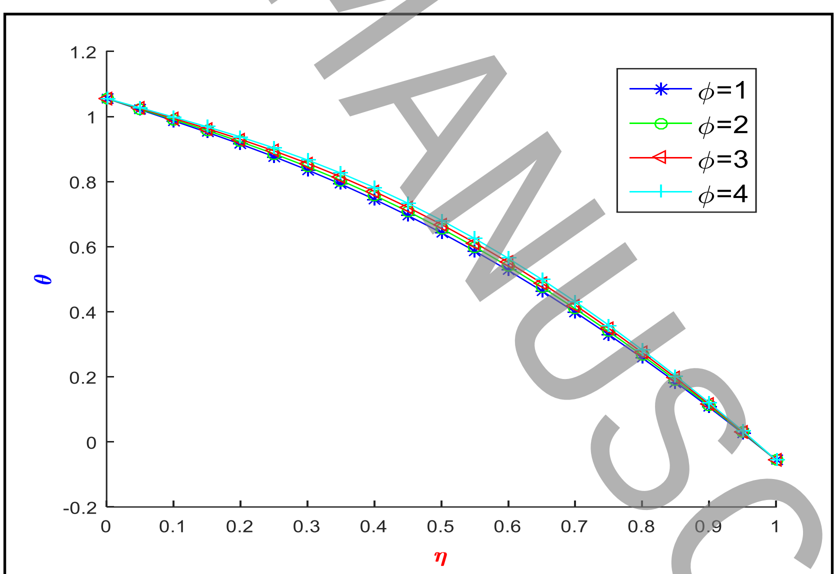

Fig. 6. Effects of nanoparticle concentration (ϕ) on temperature.

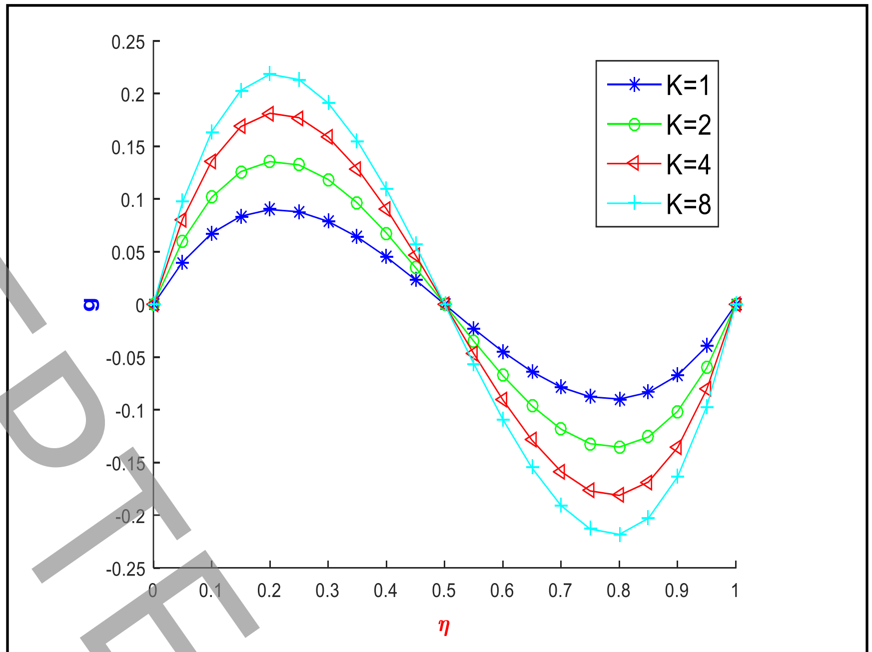

Fig. 7. Effects of micro polar (K) on rotation.

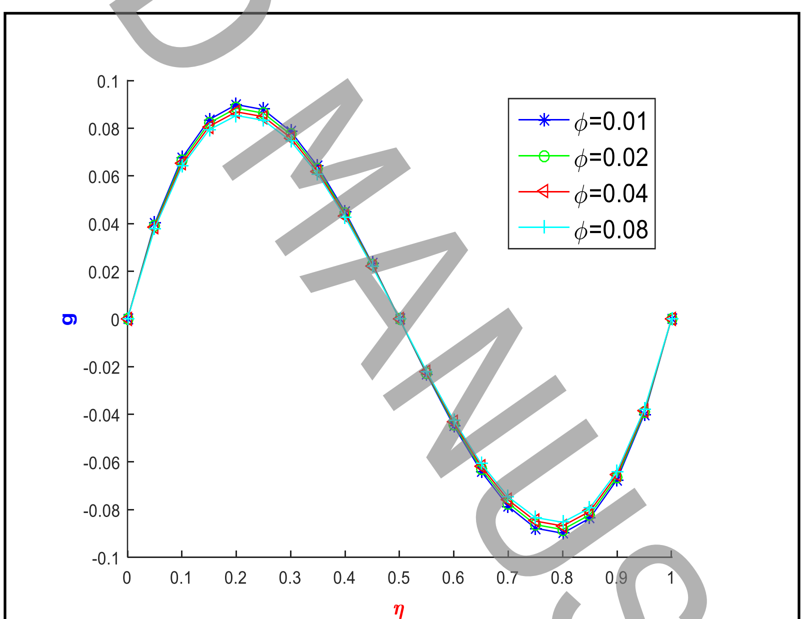

Fig. 8. Effects of nanoparticle concentration (ϕ) on rotation.

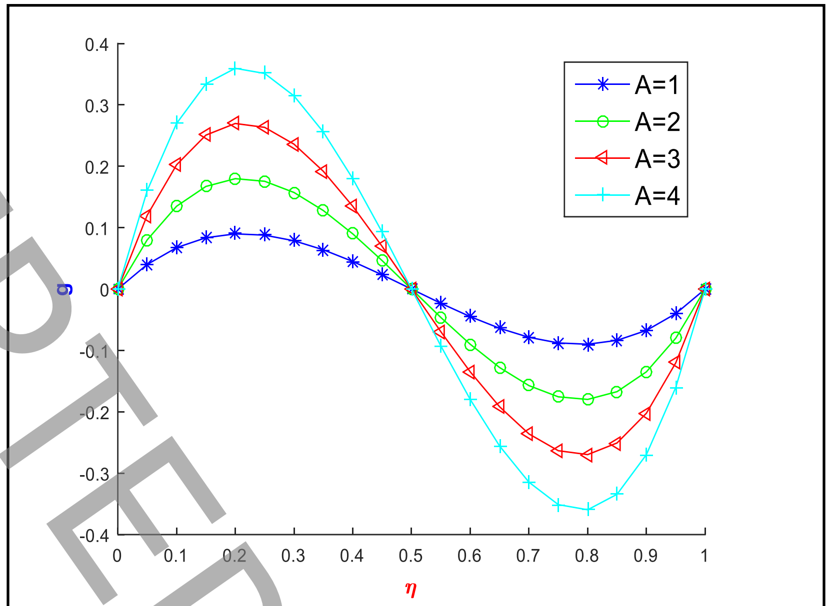

Fig. 9. Effects of A parameter on rotation.

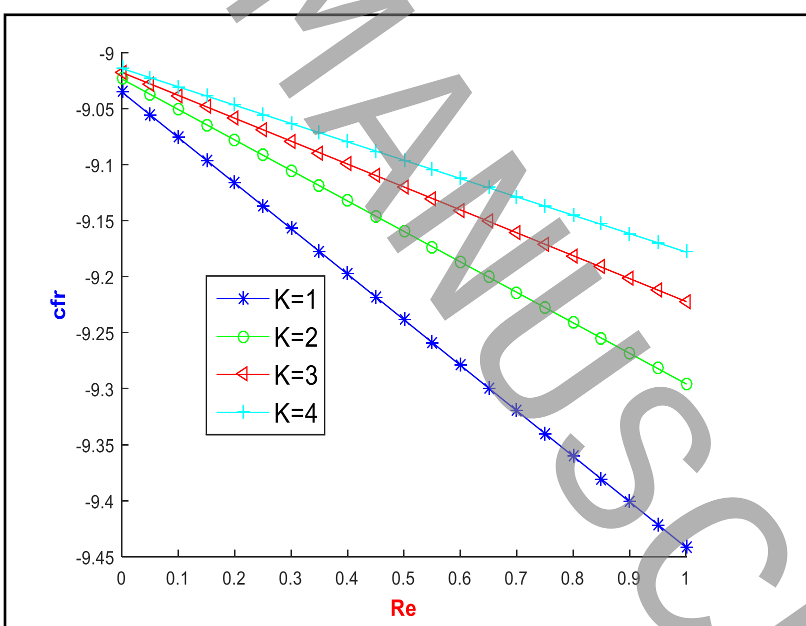

Fig. 10. Effects of Reynolds parameter (Re) and micro polar (K) on skin friction.

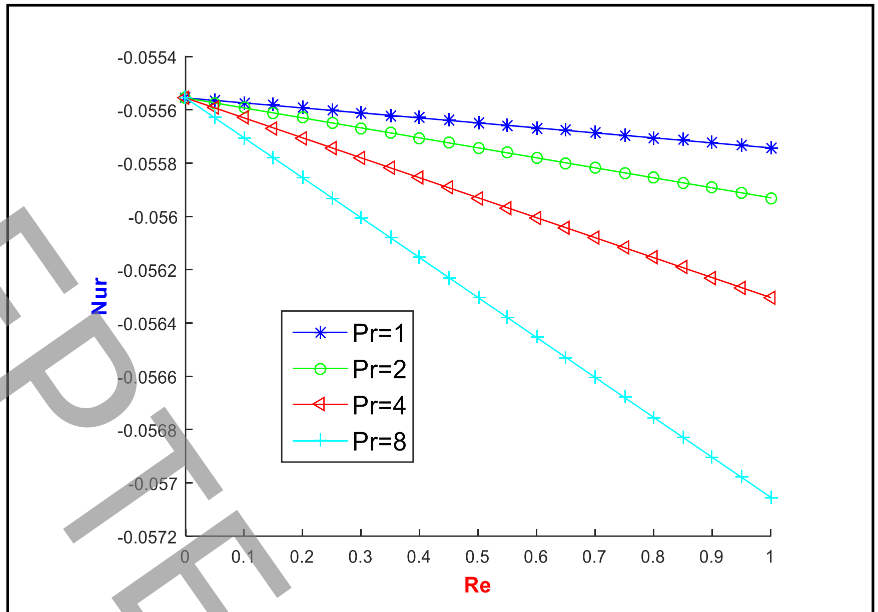

Fig. 11. Effects of Reynolds parameter (Re) and Prandtl number (Pr) on Nusselt number.

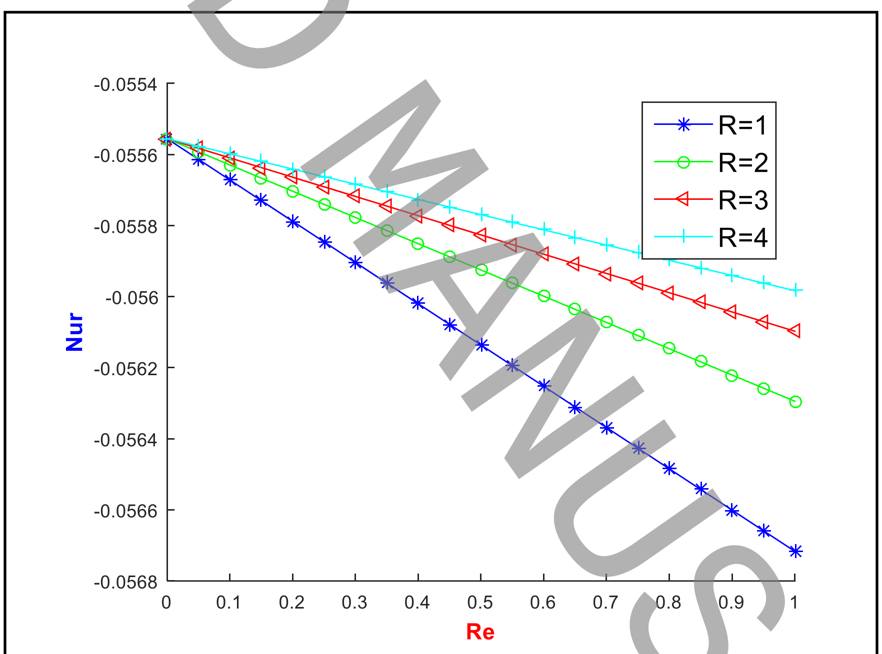

Fig. 12. Effects of Reynolds parameter (Re) and Radiation parameter (R) on Nusselt number.

Micro rotation effect of fluid molecules are represented in Figs 7-9. It is observed in Fig. 7, that micropolar parameter enhancement increases rotation of fluid molecules from the lower to the upper plate. Rotation of fluid particles surges during fluid flow as colliding motion of fluid particles abates fluid viscosity owing to increased heat dissipation. However molecules rotation of micro particles are observed to abate in Fig. 8 as concentration of nanoparticles increases from 1-8%. Temperature constant (A) effect on the micro flow rotation of rotating fluid particles are discussed in Fig. 9, this shows a surge in rotation of particles from the lower plate, however at midplate decline of fluid rotation is observed till the upper plate. As a result of thermal gradient effect at channel boundary. Skin friction effect due to movement of micropolar fluid along the boundary is seen, this shows shear stress is enhanced by improving micropolar parameter. Effect of Reynolds number is seen on the micropolar fluid flow, this reveals decline in shear stress consequently improving flow from the lower plate up to the higher plate as shown in Fig. 10. Effect of Prandtl number on the thermal transfer is seen in Fig. 11, as observed from the illustration Prandtl number abates the heat transfer process, though at a slight rate. Also Reynolds number drops as viscous force on the micropolar fluid becomes more dominant. Radiation enhancement of the micropolar fluid molecules on thermal exchange is observed in Fig. 12, this shows noteworthy improvement of heat transfer. While Reynolds effect on heat transfer reduces thermal exchange along the lower to the upper plate. Further the validation of the results are expressed in Tables 2-4 compared against fourth order Runge Kutta Fehlberg method at constant parametric values of $Re = 5, M = 2, Da = 0.1, N = 1, Pr = 2, m = 1, A = 1, K = 1, = 0.01, == 0.05$, this proves satisfactory conclusion. As observed from the Table 2, fluid transport increases steadily across the transport medium from the lower to the upper plate. Thermal exchange of fluid particles and the relating boundary is seen in Table 3, this shows the temperature at the lower plate is higher and decreases significantly as the fluid particles approaches the boundary of the lower plate surface. Rotation of micropolar fluid particles across the flow medium is expressed in Table 4, this reveals the particles moves from the lower plate and reaches its peak at the mid plate. Thereafter the fluid rotation falls as it approaches the upper plate.

Table 2. Comparison of various values of η for velocity profile.

η	RK-4 *@Re=5*	Present Work *@Re=5*	RK-4 *@Re=10*	Present Work *@Re=10*
0.0	0.0000	0.0000	0.0000	0.0000
0.1	-0.0083	-0.0083	-0.0140	-0.0140
0.2	0.0442	0.0442	0.0250	0.0250
0.3	0.1456	0.1456	0.1105	0.1105
0.4	0.2835	0.2835	0.2353	0.2353
0.5	0.4450	0.4450	0.3901	0.3901
0.6	0.6154	0.6154	0.5625	0.5625
0.7	0.7750	0.775	0.7356	0.7356
0.8	0.9116	0.9116	0.8865	0.8865
0.9	0.9945	0.9945	0.9864	0.9864
1.0	1.0000	1.0000	1.0000	1.0000

Table 3. Comparison of various values of η for temperature profile.

η	RK-4 *@Re=5*	Present Work *@Re=5*	RK-4 *@Re=10*	Present Work *@Re=10*
0.0	1.0556	1.0556	1.0556	1.0556
0.1	1.0133	1.0133	1.0822	1.0822
0.2	0.9665	0.9665	1.0997	1.0997
0.3	0.9071	0.9071	1.0919	1.0919
0.4	0.8299	0.8299	1.0487	1.0487
0.5	0.7324	0.7324	0.9648	0.9648
0.6	0.6137	0.6137	0.8385	0.8385

0.7	0.4743	0.4743	0.6708	0.6708
0.8	0.3155	0.3155	0.4642	0.4642
0.9	0.1385	0.1385	0.2215	0.2215
1.0	-0.0556	-0.0556	-0.0556	-0.0556

Table 4. Comparison of various values of η for rotation profile.

η	RK-4 *@Re=5*	Present Work *@Re=5*	RK-4 *@Re=10*	Present Work *@Re=10*
0.0	0.0000	0.0000	0.0000	0.0000
0.1	0.0674	0.0674	0.0674	0.0674
0.2	0.0899	0.0899	0.0899	0.0899
0.3	0.0787	0.0787	0.0787	0.0787
0.4	0.0450	0.0450	0.0450	0.0450
0.5	0.0000	0.0000	0.0000	0.0000
0.6	-0.0450	-0.0450	-0.0450	-0.0450
0.7	-0.0787	-0.0787	-0.0787	-0.0787
0.8	-0.0899	-0.0899	-0.0899	-0.0899
0.9	-0.0674	-0.0674	-0.0674	-0.0674
1.0	0.0000	0.0000	0.0000	0.0000

4. Conclusion

This paper investigates the micro polar fluid flow through penetrable walls under slip flow and thermal jump conditions. The rheological parameters of thermal exchange and mass transport of the micro polar fluid are studied considering transport conditions. The mechanics of the fluid are described by coupled, highly successive, nonlinear system of higher order partial differentials transformed to ordinary differentials. These are analyzed adopting the Homotopy perturbation method of analysis. Obtained results from analysis were utilized in the study of slip and thermal jump effect on micropolar fluid transport. It can be deduced from study that:

i. Quantitative increase of nanoparticles concentration from $1-4\%$ enhances thermal transfer, which effect is significant towards the lower plate.

ii. Radiation increase reveals higher heat transfer while Reynolds parameter shows reducing heat transfer.

iii. Shear stress is enhanced at the boundary due to rise in fluid vortex viscosity.

iv. Heat transfer across the transport medium improves due to radiation enhancement of rotating molecules on thermal exchange.

Results obtained was compared to Runge Kutta Fehlberg numerical method for simplified case which proved satisfactory. Study proves useful in scientific applications including tribology, arterial blood flow amongst other relevant applications.

References

[1] A.C. Eringen, Theory of Micropolar fluids, Journal of mathematical Mechanics, 16 (1966) 1-18.

[2] M.D. Aurangzaib, S. Uddin, K. Bhattacharyya, S. Shafie, Micropolar fluid flow and heat transfer over an exponentially permeable shrinking sheet, Propulsion and Power Research, 5(4) (2016) 310-317.

[3] R.N. Bank, G.C. Dash, Chemical reaction effect on peristaltic motion of micropolar fluid through a porous medium with heat absorption the presence of magnetic field, Advances in Applied Science Research, 6 (2015) 20-34.

[4] M, Sheikholeslami, M. Hatami, D.D. Ganji, Micropolar fluid flow and heat transfer in a permeable channel using analytical method, Journal of Molecular Liquids, 194 (2014) 30-36.
[5]K.S. Mekheir, S.M. Mohammed, Interaction of pulsatile flow on peristaltic motion of magneto micropolar fluid through porous medium in a flexible channel: Blood flow model, International Journal Pure and Applied Mathematics, 94 (2014) 323-339.
[6] K. Ahmad, A. Ishak, R. Nazar, Micropolar fluid flow and heat transfer over a nonlinear stretching plate with viscous dissipation, Mathematical Problems in Engineering, 13 (2013) Article ID: 257161.
[7] S. Deo, D.K. Maurya, A.N. Filippo, Influence of magnetic field on micropolar fluid flow in a cylindrical tube enclosing an impermeable core coated with porous layer, Colloid Journal , 82 (2020) 649-660.
[8] M. Trkyilmazoglu, Mixed convection flow of magnetohydramic micropolar due to a porous heater / heated deformable plate: exact solution, International Journal Heat Mass Transfer, 106 (2017) 127-134.
[9] A.T. Akinshilo, Flow and heat transfer of nanofluid with injection through an expanding or contracting porous channel under magnetic force field, Engineering Science and Technology, an International Journal, 21 (2018) 486-494.
[10] L.I. Lund, Z. Omar, I. Khan, J. Raza, E.M. Sharif, A.H. Seikh, Magneto hydrodynamic (MHD) flow of micropolar fluid with effects of viscous dissipation and joule heating over an exponential shrinking sheet: Triple solution and stability analysis, Symmetry, 12(142) (2015) 1-16.
[11] S. Ahmad, M. Ashraf, K. Ali, K.S. Nisar, Computational analysis of heat transfer and mass transfer in a micropolar fluid flow through a porous medium between permeable walls, International Journal of Nonlinear Sciences and Numerical Simulation, 52 (4) (2020) 101-113.
[12]R.A. Damseh, M.Q. Al-Odat, A.J. Chamkha, B.A. Shannak, Combined effect of heat generation or absorption and first-order chemical reaction on micropolar fluid flows over a uniformly stretched permeable surface: The full analytical solution, International Journal of Thermal Science, 48 (8) (2009) 1658-1663.
[13] M. Alizadeh, A.S. Dogonchi, D.D. Ganji, Micropolar nanofluid flow and heat transfer between penetrable walls by the presence of thermal radiation and magnetic field, Case Studies in Thermal Engineering, 12 (2018) 319-322.
[14] M.M. Rahman, I.A. Eltayeb, S. Mohammad, M. Rahaman, Thermo-micropolar fluid flow along a vertical permeable plate with uniform surface heat flux in the presence of heat generation, Thermal Science, 13(1) (2009) 23-26.
[15] A.T. Akinshilo, Investigation of nanofluid conveying porous medium through non-parallel plates using the Akbari Ganji method, Physica Scripta 95 (12) (2019) 1-11 .
[16] T. Hayat, T. Nasir, M.I. Khan, A. Alsaedi, Non-Darcy flow of water based single (SWCNTS) and multiple (MWCNTS) walls carbon nanotubes with multiple slip condition due to rotating disk, Results in Physics, 9 (2019) 390-399.
[17]S.R. Yan, R. Kalbasi, Q. Nguyen, A. Karimipour, Sensitivity of adhesive and cohesive intermolecular forces to the incorporation of MWCNTs into liquid paraffin: Experimental study and modelling of surface tension, Journal of Molecular Liquids, 310 (2020) 113235.
[18] Z. Tian, S. Rostamis, T. Taherialekouhi, A. Karimipour, A. Moradikazerouni, H. Yarmand, N.W.B.M. Zulkifli, Prediction of rheological behavior of a new hybrid nanofluid consists of copper oxide and multi walled carbon nanotubes suspended in a mixture of water and ethylene

glycol using curve fitting on experimental data, Physica A: Statistical Mechanics and Its Applications, 549 (2020) 124101.
[19] B. Sharifzadeh, R. Kalbasi, M. Jahangiri, D. Toghraie, A. Karimipour, Computer modelling of pulsatie blood flow in elastic artery using a software program for application in biomedical engineering, Computer Methods and Programs in Biomedicine, 192 (2020) 105442.
[20] M. Farzinpour, D. Toghraie, B. Mehmandoust, F. Aghadavoudi, A. Karimipour, Molecular dynamics study of barrier effects on ferro-nanofluid flow in the presence of constant and time dependent external magnetic field, Journal of Molecular Liquids, 308 (2020) 113152.
[21] S.R. Yan, R. Kalbasi, Q. Nguyen, A. Karimpour, Rheological behavior of hybrid MWCNTs-TiO_2/EG nanofluid: A comprehensive modelling and experimental study, 306 (2020) 112937.
[22]A. Zakari, M. Ghalambaz, A.J. Chamkha, D.D. Rossi, Theoretical analysis of natural convection boundary layer heat and mass transfer of nanofluids: effects of size, shape and type of nanoparticles, type of base fluid and working temperature, Advanced Powder Technology, 26(3) (2015) 935-946.
[23]A.J. Chamkha, A. Al-Mudhaf, Unsteady heat and mass transfer from a rotating vertical cone with a magnetic field and heat generation or absorption effects, International Journal of Thermal Science, 44(3) (2005) 267-276.
[24] S.H. Reddy, M.C. Raju, E.K. Reddy, Magneto convective flow of a non-Newtonian fluid through non-homogeneous porous medium past a vertical porous plate with variable suction, Journal of Applied Mathematics and Physics 4 (2016) 233-248.
[25] M. Naravhani, Unsteady free convection flow past a semi-infinite vertical plate with constant heat flux in water based nanofluids, IOP Conference Series: Materials Science and Engineering, 15, (2018) 81-94.
[26] R. Subba, R., Gorla, A.J. Chamkha, Natural convective boundary layer flow over a nonisothermal vertical plate embedded in a porous medium saturated with a nanofluid, Nanoscale and Microscale Thermophysical Engineering, 15 (2) (2010) 81-94.
[27] A.W. Xiao, H.J. Lee, I. Capone, A. Robertson, T. Wi, J. Fawdon, S. Wheeler, H.W. Lee, N. Grobert, M. Pasta, Understanding the conversion mechanism and performance of monodisperse FeF_2 nanocrystal cathode, Nature Materials , 19 (2020) 644-654.
[28] D.J. Lewis, L.Z. Zomberg, D.J.D. Carter, R.J. Macfarlane, Single crystal winter bottom constructions of nanoparticles super lattices , Nature Material, 19 (7) (2020) 719-724.
[29] H. Dessie, N. Kishan, MHD effects on heat transfer over stretching sheet embedded in porous medium with variable viscosity, viscous dissipation and heat source/sink, Ain Shams Engineering Journal , 5 (3) (2014) 967-977.
[30] S.M. Ibrahim, Radiation effects on mass transfer flow through a highly porous medium with heat generation and chemical reaction, International Scholarly Research Notices,13 (2013) Article ID 765408.
[31] B. Souyeh, M.G. Reddy, P. Sreenivasulu, T. Poornima, M. Rahimi-Gorji, I.M. Alarifi, Comparative analysis on non-linear radiative heat transfer on MHD Casson nanofluid past a thin needle, Journal of Molecular Liquids, 284 (2019) 163-174.
[32] A.T. Akinshilo, A.G. Davodi, A. Ilegbusi, M.G. Sobamowo, Thermal analysis of radiating film flow of sodium alginate using MWCNT nanoparticles, Journal of Applied and Computational Mechanics 8 (1) (2020) 219-231.

[33] A. Pantokratoras, T. Fang, Sakiadis flow with nonlinear Rosseland thermal radiation, Physica Scripta, 87 (1) (2013) 015703.
[34] H. Khan, M. Haneef, Z. Shah, S. Muhammad, S. Islam, W. Khan, The combined magneto hydrodynamic and electric field effect on unsteady Maxwell nanofluid flow over a stretching surface under the influence of variable heat and thermal radiation, Applied Science, 8 (2) (2018) 160
[35] B. Mahanthesh, B.J. Gireesha, I.L. Animasaun, Exploration of non-linear thermal radiation and suspended nanoparticles effects on mixed convection boundary layer flow on nano liquids on a melting vertical surface , Journal of Nanofluids 7 (5) (2018) 833-843.
[36] M. Mustafa, A. Mushtaq, T. Hayat, B. Ahmad, Nonlinear radiation heat transfer effects in the natural convective boundary layer flow of nanofluid past a vertical plate: a numerical study, PlosOne, 9(9) (2014) e103946.
[37] L. Dianchen, M. Ramzan, N.U. Huda, J.D. Chung, U. Farooq, Nonlinear radiation effect on MHD Carreau nanofluid over a radially stretching surface , Science Reports, 8 (2018) 3709.
[38] J.V. Ramana Reddy, V. Sugunamma, N. Sandeep, Thermophoresis and Brownian motion effects on unsteady MHD nanofluid flow over a slandering surface with slip effects, Alexandria Engineering Journal, 57 (4) (2017) 2465-2473.
[39] M.K. Nayak, F. Mabood, O.D. Makinde, Heat transfer and buoyancy-driven convective MHD flow of nanofluids impinging over a thin needle moving in a parallel stream influenced by Prandtl number, Heat Transfer—Asian Research,49 (2) (2019) 1–18.
[40] S.N.A. Salleh, N. Bachok, N. Md. Arifin, F. Md. Ali, I. Pop, Stability analysis of mixed convection flow towards moving a thin needle in nanofluid, Applied Science, 8(6) (2018) 842.
[41] P. Mohan Khrishna, R. Prakash Sharma, N. Sandeep, Boundary layer analysis of persistent moving horizontal needle in Blasius and Sakiadis magnetohydrodynamic radiative nanofluid flow, Nuclear Engineering Technology, 49 (8) (2017) 1654-1659.
[42] C. Sulochana, G.P. Ashwinkumar, N. Sandeep, Joule heating effect on a continuously moving thin needle in MHD Sakiadis flow with thermophoresis and Brownian moment , The European Physical Journal Plus, 132 (2017) 387.
[43] O. Pourmehran, M.M. Sarafraz, M. Rahimi-Gorji, D.D. Ganji, Rheological behaviour of various metal-based nano-fluids between rotating discs: a new insight Journal of the Taiwan Institute of Chemical Engineers, 18 (2018) Article ID:644800.
[44] H. Mirgolbabaee, S.T. Ledari, M. Sheikholeslami, D.D. Ganji, Semi-analytical investigation of momentum and heat transfer of a non-Newtonian fluid flow for specific turbine cooling application using AGM, International Applied Computational Mathematics, 3 (2017) S1463-S1475.
[45] A.T Akinshilo, A.O. Ilegbusi, H. Ali, A. Surajo. Heat transfer analysis of nanofluid flow with porous medium through Jeffery Hamel diverging/converging channel, Journal of Applied and Computational Mechanics, 6(3) (2020) 433-444.
[46] A.T. Akinshilo, Thermal performance evaluation of MHD nanofluid transport through a rotating system undergoing uniform injection/suction with heat generation, Bionanoscience, 9 (3) (2019) 740-748.

[47] F. Mabood, A.T. Akinshilo, Stability analysis and heat transfer of hybrid Cu-Al2O3/H2O nanofluids transport over a stretching surface, International Communications in Heat and Mass Transfer, 123 (2021) 105215.
[48] S. Shen, Application of He's variational iteration method to the fifth order boundary value problems, Journal of Physics Conference Series, 96 (2008) 012185.
[49] G. Domairry, Z. Ziabakhsh, H. Doumiri, G. Modil Habib, Approximate solution of non-Newtonian viscoelastic fluid flow on a turbine disc for cooling purpose by using Adomian decomposition method, Meccanica, 98 (2013) 4889-4909.
[50] A.S. Dogonchi, M. Alizadeh, D.D. Ganji, Investigation of MHD GO-water nanofluid flow and heat transfer in a porous channel in the presence of thermal radiation effect, Advanced Powder Technology, 28 (7) (2017) 1815-1825 .
[51] A.S. Dogonchi, D.D. Ganji, Investigation of MHD nanofluid flow and heat transfer in a stretching /shrinking convergent/divergent channel considering thermal radiation, Journal of Molecular Liquid, 220 (2016) 592-603.